Specificity and Strength of Retinogeniculate Connections

W. MARTIN USREY, JOHN B. REPPAS, AND R. CLAY REID
Department of Neurobiology, Harvard Medical School, Boston, Massachusetts 02115

Usrey, W. Martin, John B. Reppas, and R. Clay Reid. Specificity and strength of retinogeniculate connections. *J. Neurophysiol.* 82: 3527–3540, 1999. Retinal ganglion cells and their target neurons in the principal layers of the lateral geniculate nucleus (LGN) of the thalamus have very similar, center-surround receptive fields. Although some geniculate neurons are dominated by a single retinal afferent, others receive both strong and weak inputs from several retinal afferents. In the present study, experiments were performed in the cat that examined the specificity and strength of monosynaptic connections between retinal ganglion cells and their target neurons. The responses of 205 pairs of retinal ganglion cells and geniculate neurons with overlapping receptive-field centers or surrounds were studied. Receptive fields were mapped quantitatively using a white-noise stimulus; connectivity was assessed by cross-correlating the retinal and geniculate spike trains. Of the 205 pairs, 12 were determined to have monosynaptic connections. Both the likelihood that cells were connected and the strength of connections increased with increasing similarity between retinal and geniculate receptive fields. Connections were never found between cells with $<50\%$ spatial overlap between their centers. The results suggest that although geniculate neurons often receive input from several retinal afferents, these multiple afferents represent a select subset of the retinal ganglion cells with overlapping receptive-field centers.

INTRODUCTION

Neurons in the dorsal lateral geniculate nucleus (LGN) of the thalamus are the major relay for visual information traveling from the retina to the primary visual cortex. Anatomic (Hamos et al. 1987) and physiological (Cleland et al. 1971a,b; Mastronarde 1992) studies estimate that many geniculate neurons receive convergent input from two or more (up to 6) retinal ganglion cells. Given the similarities between receptive fields of neurons in the retina and LGN, several questions arise. What is the specificity and the strength of retinal inputs to geniculate neurons and to what extent do geniculate responses reflect those of the retinal cells that provide either strong or weak input?

Strong retinal inputs to an individual geniculate neuron have been studied by recording extracellularly a geniculate neuron's action potential along with its S-potential—the synaptic potential evoked by a retinal input (Bishop et al. 1958, 1962; Cleland et al. 1971b; Freygang 1958; Hubel and Wiesel 1961; Kaplan and Shapley 1984). In both cat and monkey, S-potential recordings have been used to show that geniculate neurons and their strongest retinal inputs have closely matching receptive fields, in terms of spatial location, *on* versus *off* responses, color selectivity, contrast sensitivity and X-Y classification (Hubel and Wiesel 1961; Kaplan et al. 1987; Lee et al. 1983; Reid and Shapley 1992; So and Shapley 1981). A drawback of S-potential recordings, however, is their limited ability to discriminate nondominant retinal inputs. Further, it is an untested assumption that all geniculate spikes are triggered by the S-potential being recorded. Because it is often difficult to discriminate the S-potential when associated with a spike, many spikes may occur without the S-potential and therefore in principle may be evoked by other inputs.

Both strong and weak inputs from retinal ganglion cells to geniculate neurons can be revealed using a different approach, by combining cross-correlation analysis with simultaneous recordings of monosynaptically connected pairs of neurons in the retina and LGN. Studies using this approach found that the strengths of connections between pairs of retinal ganglion cells and geniculate cells span a broad range (Cleland and Lee 1985; Cleland et al. 1971a,b; Levick et al. 1972; Mastronarde 1987, 1992; see also Arnett 1975). For some geniculate neurons, all retinal input came from single ganglion cells. For many geniculate neurons, however, only a portion of their activity was associated with each retinal input. These studies compared many features of the response properties of synaptically connected ganglion cells and geniculate cells, such as *on* versus *off* and sustained versus transient responses (Cleland et al. 1971b; Cleland and Lee 1985; Levick et al. 1972; Mastronarde 1987, 1992). Less consideration was given, however, to how the receptive fields of the two cells related to the strength of connection, or the extent to which geniculate receptive-field properties were dictated by particular retinal inputs.

Previously, we have examined how retinogeniculate transmission in the cat is modulated by temporal features in the retinal spike train (Usrey et al. 1998; see Mastronarde 1987). In the present study we examined the specificity and strength of retinal inputs to geniculate neurons. Simultaneous recordings were made from neurons in the retina and LGN of the cat that had overlapping receptive-field centers or surrounds. Quantitative receptive-field maps were made using a white-noise stimulus to compare receptive fields. Independently, cross-correlation analysis was used to determine both the presence and strength of monosynaptic connections. Results show that retinogeniculate connections are very precise; both the likelihood of connections and their strengths increase as the similarity of receptive fields increase.

METHODS

Animal preparation

All surgical and experimental procedures conformed to National Institutes of Health and U. S. Department of Agriculture guidelines and were performed with the approval of the Harvard Medical Area Standing Committee on Animals. Twelve adult cats were used. Surgical anesthesia was induced with ketamine (10 mg/kg, intramuscular)

The costs of publication of this article were defrayed in part by the payment of page charges. The article must therefore be hereby marked "*advertisement*" in accordance with 18 U.S.C. Section 1734 solely to indicate this fact.

and followed by thiopental sodium (20 mg/kg, iv, supplemented as needed). Anesthesia was maintained with thiopental sodium (2 mg · kg^{-1} · h^{-1}, iv, supplemented as needed). A tracheotomy was performed, and animals were placed in a stereotaxic apparatus. Body temperature was maintained at 37°C using a thermostatically controlled heating blanket. Temperature, electrocardiogram (EKG), electroencephalogram (EEG), and expired CO_2 were monitored continuously throughout the experiment. The nictitating membranes were retracted with 10% phenylephrine, and the eyes were dilated with 1% atropine sulfate. The eyes were refracted, fitted with appropriate contact lenses, and focused on a tangent screen located 172 cm in front of the animal. A midline scalp incision was made, and wound margins were infused with lidocaine hydrochloride. A small craniotomy was made above the LGN, and the dura was reflected.

Once all surgical procedures were complete, the animal was paralyzed with vecuronium bromide (0.2 mg · kg^{-1} · h^{-1}, iv) and ventilated mechanically. Proper depth of anesthesia was ensured throughout the experiment by *1*) monitoring the EEG for changes in slow-wave and spindle activity, and *2*) monitoring the EKG and expired CO_2 for changes associated with a decrease in the depth of anesthesia. In some animals, the paralytic agent was withdrawn to test whether the criteria adequately indicated the depth of anesthesia. At the end of each experiment, animals were given a lethal overdose of thiopental sodium (100 mg/kg).

Electrophysiological recordings and visual stimuli

Simultaneous recordings were made from retinal ganglion cells and geniculate neurons that had complete or partially overlapped receptive fields (Fig. 1). Geniculate recordings were made with a multielectrode array (Thomas Recording, Marburg, Germany; Eckhorn and Thomas 1993) consisting of seven electrodes that could be independently raised and lowered. An interelectrode spacing of 80–250 μm was achieved by advancing the electrodes through a glass guide tube (ID at tip: 300 μm) lowered to 2–3 mm above the LGN. All geniculate recordings were made from layer A of the LGN.

Retinal recordings were made intraocularly with tungsten electrodes (AM Systems, Everett, WA), which were advanced through a guide tube that penetrated the sclera of the eye (Cleland et al. 1971a; Kuffler 1953). The guide tube was inserted through an opening in a ring that was glued to the sclera and supported by a manipulator on the stereotaxic frame. Both the electrode and guide tube were attached to a ball joint and manipulator, which allowed easy access to most regions of the retina. The fundus was visualized by means of a contact lens, the power of which (−30 diopter) approximately negated the positive power of the eye's optics. With the lens in place, the fundus was in focus either by direct inspection or with a dissecting microscope (Opmi 1, Zeiss) at a normal working distance. Geniculate receptive fields were located on the retina with a laser flashed through a supplementary ocular of the microscope. The light source of the microscope was attenuated with filters so that it was in the low-mid photopic level; the laser was attenuated so that it was not much brighter than the background. With the laser as pointer, the retinal electrode could be targeted to the retinal position of the geniculate receptive fields. Once the retinal electrode was in place, the −30-diopter lens was replaced with a lens that focused the eye on the stimulus monitor, at 172 cm (so that 3 cm on the screen subtended 1°).

The arrival times and waveforms of action potentials from all eight electrodes were recorded to disk (with 100-μs resolution) by a single computer running the Discovery software package (Datawave Technologies, Longmont, CO). Spike isolation was based on off-line waveform analysis, presence of a refractory period indicated by the shape of autocorrelograms, and, in some cases, inspection of analog data recorded on tape.

Receptive fields of retinal and geniculate neurons were mapped

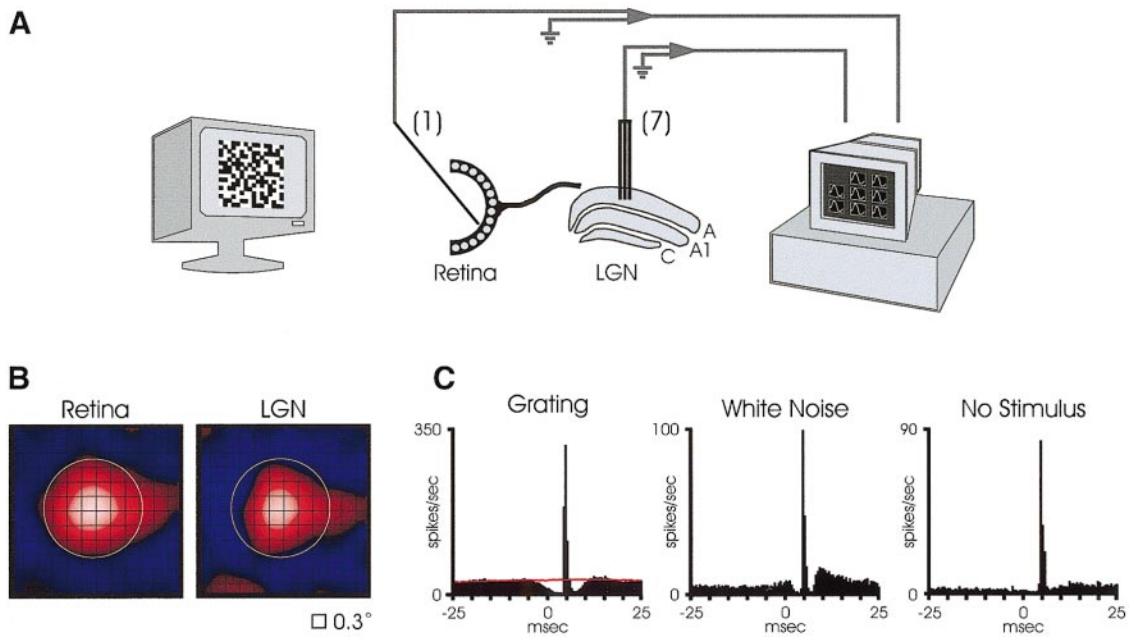

FIG. 1. Example of data from a retinal ganglion cell and geniculate neuron, recorded simultaneously, that were monosynaptically connected. *A*: experimental setup. Recordings were made in vivo with a single electrode in the intact eye and with a multielectrode in layer A of the lateral geniculate nucleus (LGN). Receptive fields were mapped with spatiotemporal white noise on a computer monitor, while data were collected. *B*: receptive fields of retinal and geniculate neurons. Red codes for *on* responses and blue for *off*. Data were smoothed by one-half pixel. The circle, drawn over both receptive fields, is from the best fitting Gaussian to the retinal receptive field (radius: 1.75 σ_{ret}). The black grid indicates the size of pixels in the stimulus array. *C*: cross-correlograms between retinal and geniculate spike trains, calculated with 0.5-ms binwidths, plotted in units of spikes per second for the geniculate neuron. Raw correlograms were divided by the total number of retinal spikes and by the binwidth, in seconds. Correlograms were calculated from data collected with grating stimulation (drifting sine-wave grating at 4 Hz), spatiotemporal white-noise stimulation, and with no stimulus (in the dark). For the grating stimulus, a shuffle-correction was calculated (red line; Perkel et al. 1967).

quantitatively by a correlation method similar to the reverse correlation of Jones and Palmer (1987) (see Citron et al. 1981; Wolfe and Palmer 1998), but using pseudorandom spatiotemporal white-noise stimuli (m-sequences; Reid et al. 1997; Sutter 1987 1992). The stimuli were created with an AT-Vista graphics card (Truevision, Indianapolis, IN) running at a frame rate of 128 Hz. The stimulus program was developed with subroutines from a runtime library, YARL, written by Karl Gegenfurtner. The mean luminance of the stimulus monitor was 40–50 cd/m^2.

The white-noise stimulus consisted of a 16 × 16 grid of squares (pixels) that were white or black one-half the time, as determined by an m-sequence of length $2^{15} - 1$. The stimulus was updated either every frame of the display (7.8 ms) or every other frame (15.6 ms). The entire sequence (~4 or 8 min) was often repeated several times. Pixels were either 0.6 or 0.3° on a side. This was small enough to map receptive fields, which were between 5 and 25° eccentricity, at a reasonable level of detail. In most cases 8–16 pixels filled the center of a cell's receptive field.

In many cases, sinusoidal grating visual stimuli were also used to characterize the neurons under study. In particular, in cases for which the X-Y classification was uncertain, a modified null test was performed with contrast-reversing gratings at several spatial frequencies (Enroth-Cugell and Robson 1966; Hochstein and Shapley 1976). Because we often recorded from a number of X and Y cells in the LGN simultaneously, the differences in the receptive-field sizes usually allowed for an unambiguous classification without a null test. At each eccentricity, all X cells had similar sizes as mapped with white noise, and the Y cells were two to three times larger (Linsenmeier et al. 1982). Although geniculate cells were not classified explicitly as lagged or nonlagged (Saul and Humphrey 1990), the majority had similar impulse responses (see later description) and were almost certainly nonlagged.

Once receptive fields were mapped with white-noise stimuli, large numbers of spikes (usually, more than 50,000 retinal spikes, 20,000 geniculate spikes) were collected using a drifting sine-wave grating, during subsequent runs of the white-noise stimulus, and in the absence of any stimulus (eyes covered). These spike trains were used for cross-correlation analysis.

Data analysis

CROSS-CORRELATION ANALYSIS. Cross-correlograms between retinal and geniculate spike trains were made to examine connectivity between pairs of cells. Peaks indicative of monosynaptic connections (*monosynaptic peaks*) were analyzed in two ways (Reid and Alonso 1995). First, a statistical test assessed whether peaks that had the time course associated with monosynaptic connections (Cleland et al. 1971a,b) were significant. Second, the magnitude and time course of statistically significant peaks was measured. For all quantitative analysis, correlograms were calculated between −10.0 and +10.0 ms, with 0.1-ms time bins. To display a longer baseline, the correlograms shown in Figs. 1 and 2 are between −25.0 and +25.0 ms with 0.5-ms time bins. For most pairs of cells, cross-correlograms were made with data collected both during white-noise stimulation and during stimulation by sine-wave gratings drifting at 4 Hz. Shuffle-subtractions were made with data collected with drifting gratings, to remove the stimulus-dependent portion of the correlations (Perkel et al. 1967).

Significance of correlogram peaks was assessed with the method of Reid and Alonso (1995). First, the cross-correlograms were band-pass filtered, with Butterworth filters that decreased to 50% outside of the range 500 Hz to 1.5 kHz, and to 10% outside the range 350 Hz to 2.1 kHz. This very high-frequency range was used because the peaks in the correlograms averaged ~0.6 ms, full width at half-maximum (see later description). This procedure entirely eliminated the stimulus-dependent portion of the correlation (high-pass) and decreased some of the noise due to the 0.1-ms binwidth (low-pass). The standard deviation of the baseline was calculated from the filtered correlograms between −10.0 and +10.0 ms, after removal of the interval between 2.0 and 5.0 ms. If any one of the 30 bins between 2.0 and 5.0 ms was >4 standard deviations above the baseline noise, the correlation was judged significant. The method relies on the fact that the correlations examined are many times faster than any stimulus-dependent portion of the correlation. Shuffle-subtraction is therefore not necessary, and the method can be used on data collected with a nonperiodic stimulus, such as white noise. It also rejects slower, stimulus-independent correlations that could come from sources other than monosynaptic connections (such as slower intraretinal correlations: Mastronarde 1983a,b, 1989; Meister et al. 1995). Finally, it may reject correlations from retinal input to interneurons, which have been found to be significantly slower (Table 1 in Mastronarde 1992).

The strengths of correlations were calculated from the raw, unfiltered correlograms. The correlogram represents the number of occurrences of paired events at each delay between retinal and geniculate firing. The *peak interval* was taken as 1.2 ms on either side of the highest single bin, which was constrained to fall in the range between 2.0 and 5.0 ms. The *baseline* was defined as the average rate at 2.0 ms on either side of the peak interval. The *peak magnitude* was defined as the integral of the correlogram, minus the baseline, over the peak interval. We then calculated two measures of correlation strength: *efficacy* and *contribution* (Levick et al. 1972). Efficacy is the peak magnitude normalized by the number of retinal (presynaptic) events. Contribution is the peak magnitude normalized by the number of geniculate (postsynaptic) events. To the extent that the peaks were caused by monosynaptic connections, the efficacy and contribution have very simple interpretations. Efficacy represents the fraction of the retinal spikes that caused the geniculate neuron to fire. The contribution represents the fraction of the geniculate spikes that were caused by a spike from the retinal neuron.

The baseline we have chosen to calculate efficacy and contribution is different from the baseline obtained by subtracting the shuffle-correlogram (Perkel et al. 1967). In general, the shuffle-correlogram is taken as the component of the cross-correlogram due to the indirect influence of the stimulus and not to direct neural interactions. In cases in which correlations are very strong, however, this is not the case. For instance, in the case of a geniculate neuron that receives all its input from a single retinal cell, the peak in the correlogram would contain one count for each geniculate spike. A zero baseline should therefore be subtracted from the raw correlogram to get the correct answer of 100% contribution, but the shuffle-correction would subtract a nonzero baseline. We avoided this problem by taking the baseline from the raw correlogram itself, 2.0 ms on either side of the peak (also see Mastronarde (1987) for justification of this choice of baseline). Because of the refractory period of the retinal neuron, the baseline calculated in this manner declined to nearly zero in the case of a very high contribution (for instance, in pair 12, Fig. 2), even though the shuffle-correlogram (shown as a red line over the histogram) was nonzero. For weaker contributions (for instance, in pair 1), however, the baseline calculated in this manner was almost always the same as would have been obtained with the shuffle-correlogram.

Receptive-field mapping: reverse correlation

Spatiotemporal receptive-field maps (kernels) were calculated from the responses to the white-noise stimulus by a correlation method (Reid et al. 1997; Sutter 1987, 1992; see Citron et al. 1981; Jones and Palmer 1987; Wolfe and Palmer 1998). For each delay between stimulus and response and for each of the 16 × 16 pixels, we summed the stimuli that preceded each spike. In this calculation, the bright phase is assigned the value +1, the dark phase −1. When normalized by the total duration of the stimulus, the result is expressed in units of spikes per second. For each of the pixels, the kernel can also be thought of as the average firing rate of the neuron, above or below the mean, after the bright phase of the stimulus at that pixel. This time course is called the *impulse response* of the neuron at a given pixel.

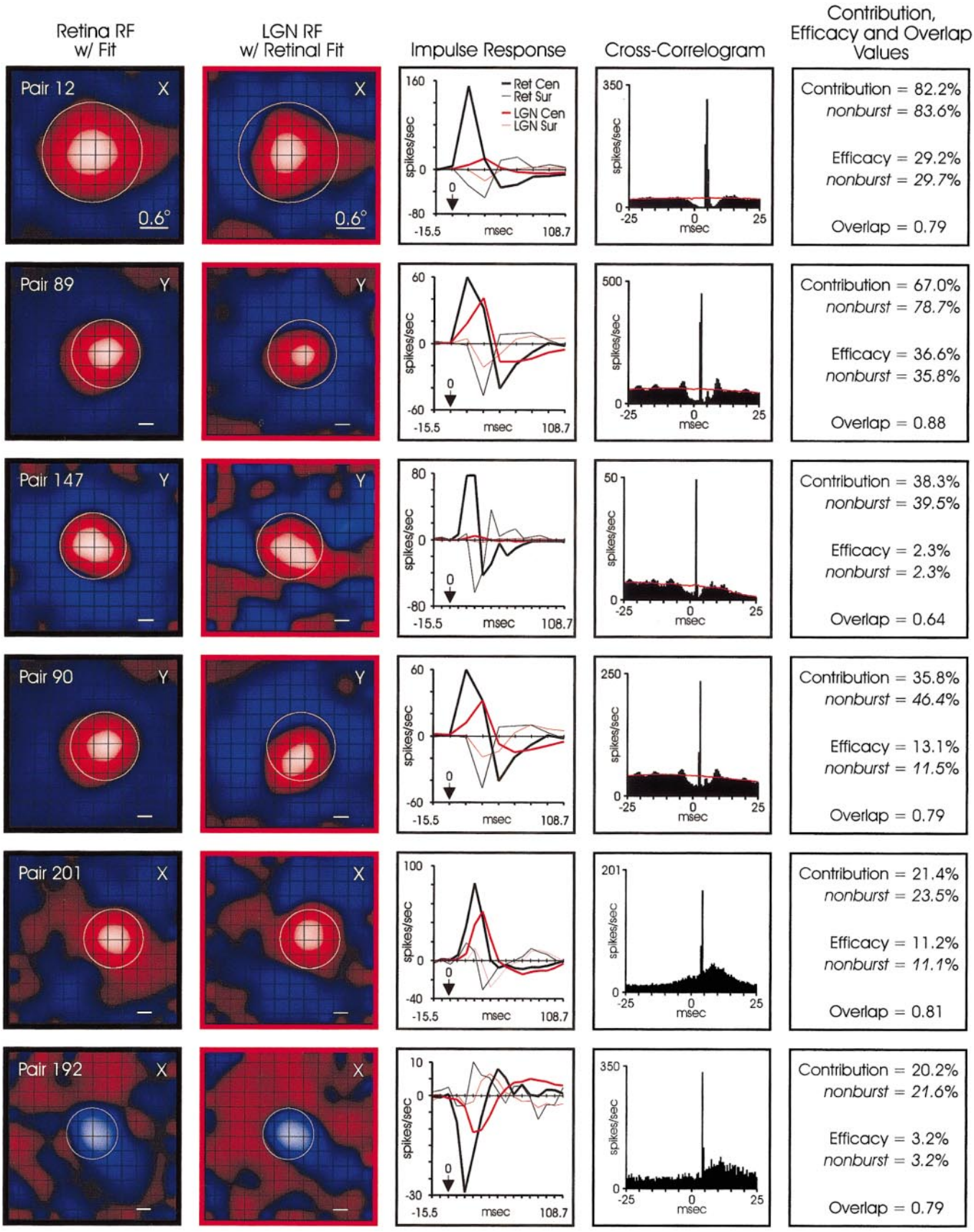

FIG. 2. Receptive fields and cross-correlograms from all pairs of cells that met the criteria for a monosynaptic connection. *Columns 1* and *2* (columns are numbered from the *left*): receptive field plots of retinal and geniculate neurons, with circles corresponding to retinal centers (radius: 1.75 σ_{ret}), as in Fig. 1. All scale bars correspond to 0.6°. Pairs in our sample were numbered from 1 to 205. Here, they are ordered according to their contribution values. Retinal recordings were made from regions of the right eye that project to layer A of the left LGN (exact visual coordinates were not documented). *Column 3*: visual impulse response functions of retinal (black lines) and geniculate neurons (red lines). Center responses are plotted with thick lines, surrounds with thin lines. Responses

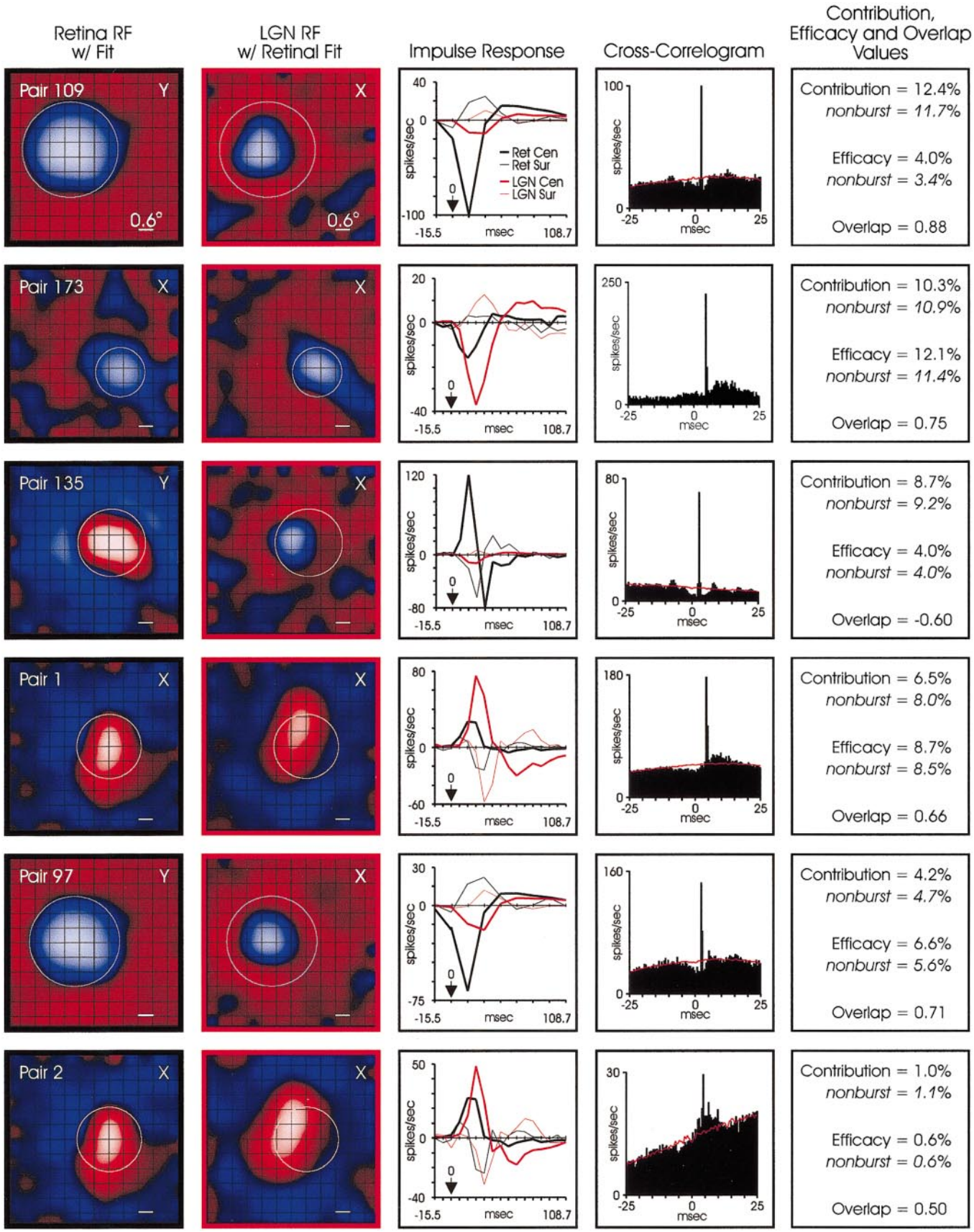

FIG. 2. (*continued*) are plotted as the increase or decrease in firing after the bright phase of the stimulus (indicated by arrows at *time 0*). Bin widths on the x-axis correspond to rates of stimulus presentation (see METHODS). *Column 4*: cross-correlograms between retinal and geniculate spike trains, as in Fig. 1. When grating stimulation was used, the shuffle correction is shown in red, otherwise, white-noise stimulation was used. *Column 5*: contributions and efficacies, calculated from the cross-correlograms, and overlap, calculated from the receptive field maps (see METHODS). The nonburst contributions and efficacies were calculated from geniculate spike trains after the later spikes in bursts were removed. Ret, retinal; cen, center; sur, surround.

For most purposes, time was binned at the stimulus update period (1 or 2 display frames, which corresponds to 7.8 or 15.6 ms). The zero bin corresponds to the average stimulus at the time of each spike; neurons with latencies of <15.6 ms therefore show responses in the zero bin. The 15.6 ms bin corresponds to the responses with latency between 15.6 and 31.2 ms, and so on. To quantify certain parameters, in particular t_{max} (defined later), the responses were sampled in 1.9-ms bins.

To assess the time course and magnitudes of both center and surround responses, it was necessary to identify the pixels in the receptive-field center. First, the largest single response in the spatiotemporal receptive field was located. This maximum defined the position of greatest sensitivity at the best delay between stimulus and response. Next, the spatial receptive field was averaged over a range of times (31.2 ms total, or 4 display frames) before and after the best delay, to define the *spatial receptive field*. This definition is somewhat arbitrary: because the time courses of the center and surround responses are different, a different set of conventions would give a different spatial receptive field. The *center* was defined as all contiguous spatial positions in this spatial receptive field that were the same sign as the strongest response and were >2 SD above the baseline noise. The baseline noise was taken as the standard deviation of the kernel values for all pixels and for delays (54.4–108.7 ms) that were well beyond the peak response. The *surround* was defined as all other points that were within a certain distance of the center. The surround width (in pixels) depended on the number of pixels in the center (N_{center},) according to the following formula: $3 + (N_{center})^{1/2}$. Thus there was a minimum width of the surround, and it increased roughly linearly with the diameter of the center. The impulse responses of all of the pixels in the center and surround were added together to yield the *center impulse response* and *surround impulse response*, respectively (Fig. 2). The definition of center and surround are, again, somewhat arbitrary, but it should be noted that several others were tried and none of the results presented were critically dependent on the exact definition.

Parameters quantifying the impulse responses were calculated as follows. The time of maximum response, t_{max}, was calculated from the center impulse response, sampled in 1.9-ms bins. The *rebound time*, $t_{rebound}$, was defined as the first time, after t_{max}, that the response was opposite in sign from the maximum response. The *response magnitude*—which quantifies the first phase of the response, the response before the rebound—was defined as the integral of the impulse response for all times before $t_{rebound}$. Finally, the *rebound magnitude* was defined as the integral of the impulse response for times greater than $t_{rebound}$ (up to 108.7 ms).

Overlap between retinal and geniculate receptive fields was assessed in two ways. First, the size and location of the centers were quantified by fitting the best *single* two-dimensional Gaussian to the spatial receptive field. Note that for the purpose of determining relative size and overlap, a difference of Gaussian model (Rodieck 1965) was not used. In a difference of Gaussian fit, the center size is somewhat dependent on the surround parameters and is less tightly constrained than if the surround is ignored. Empirically, we found that a circle drawn at 1.75 space constants (σ, or standard deviations) from the peak of the best fitting Gaussian roughly corresponds to the spatial extent of the receptive field center (Figs. 1 and 2). Note that a different convention was used in Reid and Alonso (1995) and Alonso et al. (1996); here we used the expression $A \exp(-|\mathbf{x} - \mathbf{x_c}|^2/\sigma^2)$, whereas previously we used $A \exp(-|\mathbf{x} - \mathbf{x_c}|^2/2\sigma^2)$. A is the amplitude, $\mathbf{x_c}$ the center, and σ the standard deviation of the Gaussian.

Overlap was also assessed in a model-independent way. First, each spatial receptive field was normalized so that the dot product with itself was one (the dot product of two receptive fields is equal to the product of the values at each pixel, summed over all pixels). *Overlap* was defined as the dot product of the two different receptive fields, after normalization. The value for overlap can therefore range between −1 and +1. If the spatial receptive fields were identical to within a scale factor, then the overlap would be +1. If they were identical, but with opposite sign—one *on*-center, the other *off*-center—then the overlap would be −1. Imperfectly overlapped or dissimilar receptive fields would yield smaller values (see Fig. 2 for examples).

RESULTS

In total, we recorded the responses of 205 pairs of retinal ganglion cells and geniculate neurons with overlapping receptive-field centers or surrounds. Of the 205 pairs, 12 displayed statistically significant peaks in their cross-correlograms; these peaks indicated the presence of a monosynaptic connection (see METHODS).

Comparing receptive fields and assessing connectivity

The receptive fields of retinal ganglion cells and geniculate neurons were mapped with white-noise stimuli (Fig. 1*B*) and connectivity between them was assessed with cross-correlation analysis (Fig. 1*C*). The two panels of Fig. 1*B* show the receptive fields of a pair of *on*-center–*off*-surround X cells, recorded from simultaneously in the retina and LGN. Regions of a cell's receptive field that responded to the bright phase of the stimulus (*on* responses) are shown in red and regions that responded to the dark phase (*off* responses) are shown in blue. The circle over the retinal ganglion cell's receptive field is drawn at 1.75 space constants from the peak of the Gaussian that best fitted the center response. The same circle is also shown superimposed on the geniculate cell's receptive field to allow further comparison of the degree of overlap between the two receptive fields. In this example, the two cells have nearly identical receptive fields, with the exception that the center of the retinal ganglion cell's receptive field is slightly larger than that of the geniculate cell.

Cross-correlation analysis was used to determine whether pairs of simultaneously recorded retinal and geniculate neurons were monosynaptically connected. The cross-correlograms shown in Fig. 1*C* show the relationship between the retinal and geniculate cells' firing patterns under different stimulus conditions. Zero in the correlograms indicates the time a retinal spike occurred and the narrow peak, ~4.5–5.0 ms to the right of zero, indicates that the geniculate cell often fired in response to a retinal spike. This narrow, short-latency peak is taken as evidence of a monosynaptic connection (Cleland et al. 1971a,b). Although spike rate varied depending on the stimulus used, the peak in each cross-correlogram retained its latency, narrow width, and rapid rise and fall under conditions of either grating or white-noise stimulation, as well as in the absence of a stimulus (spontaneous activity, eyes covered).

Receptive fields, impulse response functions, and cross-correlograms for each of the 12 pairs of connected retinal ganglion cells and geniculate neurons are shown in Fig. 2. *Column 1* of Fig. 2 (columns are numbered from the *left*) shows the receptive fields of each of the 12 retinal ganglion cells. As in Fig. 1, circles drawn at 1.75 space constants (σ_{ret}) from the peak of the center response are shown superimposed on the retinal receptive fields. The same circles are also shown superimposed over the simultaneously recorded geniculate cell's receptive field (Fig. 2, *column 2*) to aid comparison of locations and sizes of receptive fields.

Receptive-field overlap was further quantified with a nor-

malized dot product (see METHODS) for each of the 12 pairs of cells (Fig. 2, *column 5*). For most cell pairs, retinal and geniculate receptive fields were well overlapped. Eleven of the 12 pairs had positive overlap values that ranged from 0.88 (very precise overlap, same sign) to 0.50 (less overlap, same sign). Pair 135 had a negative value of −0.60 because the centers overlapped, but the retinal cell was *on*-center and the geniculate cell was *off*-center.

Although most cell pairs had corresponding X or Y classification, three pairs of cells were nonmatching. Pair 135, in addition to its *on-off* mismatch, was a mismatched retinal Y cell connected to a geniculate X cell. Pairs 97 and 109 were from a single retinal Y cell with connections to two different geniculate X cells. Despite the X-Y mismatches of these two pairs, their receptive fields were well overlapped and were all *off*-center. Although the occurrence of X-Y mismatches may seem surprising, it should be noted that previous anatomic and physiological studies have also found X-Y mismatches between retina and LGN (Hamos et al. 1987; Mastronarde 1992).

The time course of visual responses of pre- and postsynaptic neurons are plotted in *column 3* of Fig. 2. These *impulse responses*, shown for both centers and surrounds, were derived from the spatiotemporal receptive fields as outlined in METHODS. They can be thought of as the average response to the bright phase of the stimulus, summed over all of the pixels in either the center or the surround. Because the stimulus was binary—that is, if a pixel was not light, it was necessarily dark—a negative response to the bright stimulus (seen for the *off*-center neurons) is formally equivalent to a positive response to the *dark* phase of the stimulus.

A number of points can be appreciated from the impulse responses. First, the impulse responses of the geniculate receptive-field centers (red thick lines) are usually of lower amplitude and are delayed with respect to the retina centers (black thick lines). Second, the impulse responses of both the geniculate and retinal centers have an overshoot, or rebound, that begins at ~40 ms. The rebounds tended to be greater for Y cells than X cells, as would be expected (Cleland et al. 1971b; Ikeda and Wright 1972; see later discussion), and were also stronger for neurons in LGN than in the retina. Note finally that the surrounds also tended to be relatively stronger in the LGN. All of these qualitative points, some of which are hard to appreciate in Fig. 2, will be examined quantitatively (Fig. 3).

Finally, for each of the 12 positive correlations, we calculated two values (Fig. 2, *column 5*) that quantify the influence of a presynaptic cell on the firing of its postsynaptic target: *efficacy* and *contribution* (Levick et al. 1972; see METHODS). Efficacy refers to the percentage of presynaptic spikes that evoke a postsynaptic spike; contribution refers to the percentage of postsynaptic spikes that are due to these presynaptic spikes (assuming strict causality). Cell pairs in Fig. 2 are shown ordered according to their contribution values. Although earlier studies with dual recordings in the retina and LGN reported that 8% of cell pairs were completely driven by a single retinal input (Cleland et al. 1971a,b; Levick et al. 1972; cf. Cleland and Lee 1985 and Mastronarde 1992 who found higher percentages), none of the retinal cells in the present study provided 100% contributions to a given geniculate neuron. Of the 12 pairs of connected cells in our study, contribution values ranged from 1 to 82%, and efficacy values ranged from 0.6 to 36%.

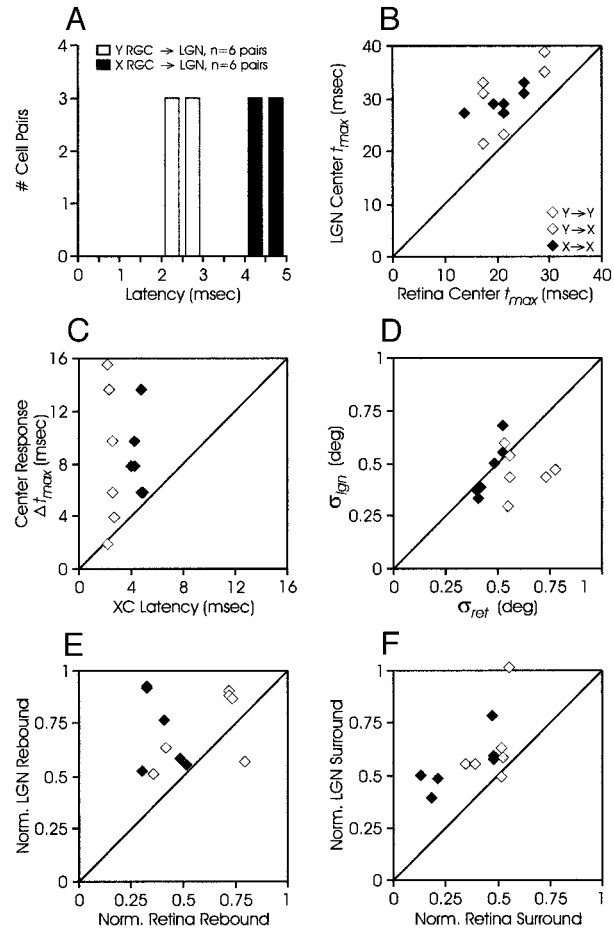

FIG. 3. Quantification of synaptic latencies and differences between retinal and geniculate visual responses. *A*: synaptic latencies for X and Y retinal neurons. *B*: relative timing of peak visual response for geniculate versus retinal center mechanisms. Solid diamonds: X → X; shaded: Y → X; open: Y → Y. *C*: comparison between synaptic latencies (from A) and relative visual delays between retina and LGN. *D*: center size comparison from best-fitting Gaussian to retinal and geniculate receptive fields. *E*: comparison of the relative sizes of the rebounds in the retinal and geniculate impulse responses. Rebound magnitudes were normalized by the initial response magnitudes (see METHODS). *F*: comparison between the surround magnitudes (normalized by center magnitudes) between retina and LGN. RGC, retinal ganglion cell.

The distribution of contributions reported here is somewhat skewed toward lower values (Fig. 2, see Fig. 6*C*) compared with those reported in previous studies (Levick et al. 1972; Mastronarde 1987, 1992). For instance, Levick and colleagues (1972) found in their study that aside from the 8 of 105 cell pairs that had contribution values of 100%, "the sample of contributions was distributed more or less evenly from 3% up." The difference is probably because, whereas they seemed to have searched for connected pairs, we used a multielectrode to study a large number of geniculate neurons, irrespective of whether they were connected to a given ganglion cell. For this reason, we may have uncovered more examples of weak connections. Sampling bias is almost certainly another important factor; for instance, we found very few lagged cells in the LGN, a class that was shown by Mastronarde (1987) to be driven by a single retinal input.

Another possible explanation for the lower contribution values reported here is based on bursts in the geniculate spike train. Specifically, although a single retinal spike may evoke a

burst of action potentials in a geniculate neuron, only the first spike falls in the time interval we used to measure correlation strength (see METHODS). Many factors can affect geniculate bursts including arousal, depth and type of anesthesia, and cortical feedback (Guido and Weyand 1995; Hubel 1960; Livingstone and Hubel 1981; Mukherjee and Kaplan 1995; Sherman 1996; Sherman and Koch 1986; Steriade et al. 1993). We used the criteria of Sherman and colleagues (Guido et al. 1992; Lu et al. 1992) to identify geniculate bursts and then replaced each burst with a single event located at the time of the burst's first action potential. Efficacy and contribution values from burst-subtracted spike trains are given (Fig. 2, *column 5*) below the corresponding values calculated from nonsubtracted spike trains. When bursts were subtracted, contribution values increased only slightly (by 8.5 ± 8.0%, mean ± SE) and none of the pairs in our sample reached 100% contribution. Finally, because burst-subtraction removed geniculate spikes, efficacy values decreased slightly (by −6.4 ± 7.2%).

Similarities and differences between retinal and geniculate responses

As can be appreciated qualitatively from Fig. 2, the receptive fields of pre- and postsynaptic neurons were subtly different in several ways. To quantify the relations between them, we analyzed the impulse responses of both centers and surrounds and derived several parameters related to their strength and timing. To understand the differences between the time courses of retinal and geniculate visual responses, we first considered whether these differences may be caused by a simple synaptic delay.

In a strictly feedforward system, the location of the correlogram's peak can be thought of as the latency: the delay between pre- and postsynaptic responses. Factors affecting latency include conduction velocity, synaptic transmission and postsynaptic spike generation. The range of latencies between retinal and geniculate responses for the 12 pairs was 2.3–4.9 ms. In all cases, the peaks were extremely narrow: the rise from half-maximum was 0.23 ± 0.05 (mean ± SE) ms and the decay to one-half maximum was 0.33 ± 0.09 ms. The correlation between latency and the retinal cell's X-Y classification was extremely tight (Fig. 3*A*). Consistent with previous reports that describe faster conduction velocities for Y-cell axons than X-cell axons (Cleland et al. 1971b; Fukada 1971), Y cells in our sample had shorter latencies (2.66 ± 0.49 ms) between pre- and postsynaptic response than did X cells (4.45 ± 0.36 ms).

As noted, the time course of the maximum *visual* response of the geniculate neurons was delayed relative to the retinal ganglion cell. To demonstrate this quantitatively, we plotted the geniculate t_{max} (time of maximum visual response, see METHODS) versus the retinal t_{max} (Fig. 3*B*). The retinal t_{max} ranged between 13.4 and 29.1 ms; the LGN t_{max} ranged between 21.4 and 38.8 ms. In each case the LGN t_{max} was greater than the retinal $t_{max,}$ so all points fell above the line of unit slope. A similar relationship held for the time of maximum visual response of the surrounds (not shown). In fact, the change in the timing of the surround was less than the change in center timing in most cases. Given the relative noisiness of the surround measurements, however, it is unlikely that this effect is significant. In Fig. 3*C* the change in center timing between retina and LGN (Δt_{max}) is plotted versus the latencies from Fig. 3*A*. The change in center timing (1.9–15.5 ms) was in most cases significantly longer than the synaptic delay between pre- and postsynaptic neurons (again, 2.3–4.9 ms). Thus, the delayed geniculate visual responses were not solely due to the latency between retinal and geniculate firing. It is possible, however, that they were caused by slower interactions between spikes from the retinal afferent, which can last for tens of milliseconds (Mastronarde 1987; Usrey et al. 1998).

It had been noted that retinal receptive-field centers are larger than those of their geniculate targets (Cleland and Lee 1985; Cleland et al. 1972a). To assess this, we compared the space constants from the two-dimensional Gaussian fits: σ_{ret} and σ_{LGN} (Fig. 3*D*; note that in Figs. 1 and 2, the plotted circles have a radius of 1.75 σ_{ret}). When the three examples of a Y cell connected to an X cell are discounted, there were few consistent differences between the retinal and geniculate centers.

Although the spatial extent of the center changed little between retina and LGN, we found evidence of increased spatial and temporal antagonism in the LGN. By temporal antagonism, we mean the rebound seen in the impulse response. This rebound can be related to a more conventional measure—*transience* (Cleland et al. 1971b; Ikeda and Wright 1972)—in the following way. Transience is normally measured by recording the response to a step function, to yield the *step response*. Instead of measuring step responses directly, we studied the time course of visual responses with white noise. The time course of the responses as measured with white noise approximates the response to a brief impulse, the impulse response. Because a step function can be thought of as the integral of an impulse, the step response (assuming linear temporal summation) should be the integral of the impulse response (Fig. 2, *column 4*). Therefore the magnitude of the rebound should be directly related to the transience of the neuron's response to step stimuli (see Gielen et al. 1982).

Quantification of the rebound indicated that it was significantly greater for most retinal Y cells than for retinal X cells (Fig. 3*E*, open and shaded diamonds), as would be expected from the greater transience of Y cells (Cleland et al. 1971b; Ikeda and Wright 1972). Further, for all cases except one, in which a retinal Y cell connected to a geniculate X cell, the rebound in the geniculate was greater than in the retina (Fig. 3*E*). This demonstration of more transient responses in the LGN is in agreement with studies of the responses to localized stimuli (Cleland and Lee 1985); it is also consistent with the more band-pass temporal frequency tuning and phase advances found in the LGN (Kaplan et al. 1987; Mukherjee and Kaplan 1995).

The relative strength of center and surround was quantified by normalizing the magnitude of the surround response by the center response magnitude (see METHODS). The normalized retinal surrounds ranged from 0.07 to 0.49, whereas the geniculate surrounds ranged from 0.39 to 1.01. In all cases but one, the geniculate surround was stronger than the retinal surround (Fig. 3*F*). This finding is consistent with the original report of increased surround antagonism (Hubel and Wiesel 1961) and is confirmed by subsequent extracellular (Levick et al. 1972) and intracellular recordings made in the LGN (Singer and Creutzfeldt 1970; Singer et al. 1972), although it has not been consistently found in all studies (So and Shapley 1981). The different degrees of spatial antagonism found between studies may be the result of differing states of anesthesia of the

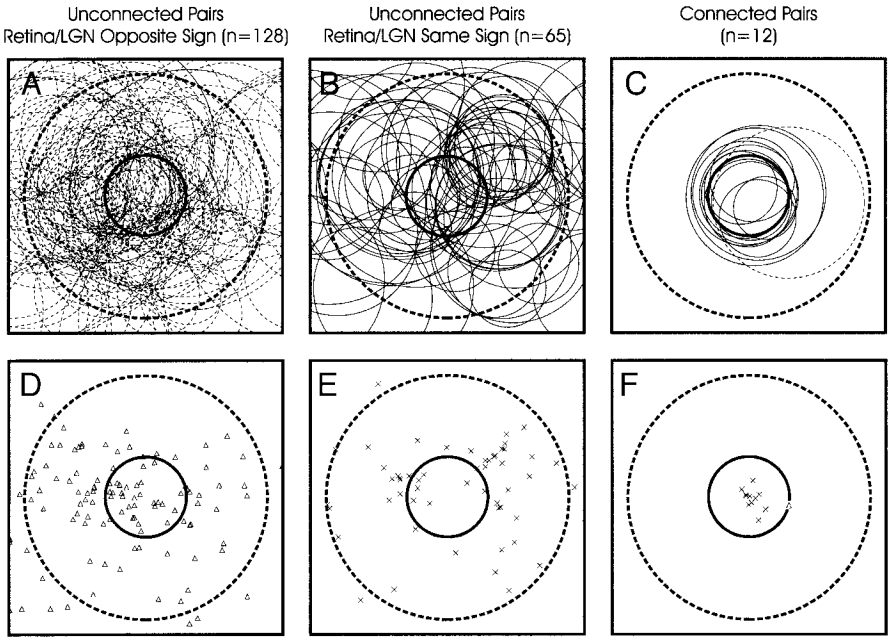

FIG. 4. Summary of overlap of unconnected pairs with opposite (*on* versus *off*) response signs (*A*, *D*), unconnected pairs with the same response sign (*B*, *E*), and connected pairs (*C*, *F*). The thick circle in each panel corresponds to the LGN receptive-field center; the surround is shown schematically with a thick dotted line. *A*, *B*, *C*: relative position and size of retinal receptive field centers are indicated by thin circles: solid for same-sign centers, dashed for opposite-sign centers. The geniculate center (thick line) has a radius of 1.75 (all units are normalized, therefore dimensionless). The distance between the geniculate center and the retinal center for each pair is equal to the actual distance, divided by σ_{lgn}; the diameter of the thin circles is 1.75 $\sigma_{ret}/\sigma_{lgn}$. *D*, *E*, *F*: relative position of retinal receptive field centers are shown without indicating their size. × same-sign center; triangle, opposite-sign center.

animals; anesthesia has been shown to profoundly affect the degree of band-pass temporal tuning of LGN cells (Mukherjee and Kaplan 1995), which is presumably also the result of inhibitory interactions.

Specificity and strength of retinogeniculate connections

To examine how the probability of finding a retinogeniculate connection depends on receptive-field overlap, we used two procedures to characterize the relationship between the retinal and geniculate receptive fields: a Gaussian fit to the receptive field centers and a normalized dot product between the two receptive fields.

The Gaussian fits allowed the relative position and size of the two receptive fields to be compared. To compare the relationship between all cell pairs, we normalized the distance between receptive fields, as well as both space constants (σ_{ret} and σ_{lgn}), by σ_{lgn}. We used this procedure to analyze the spatial relationship between the receptive-field centers of all of the unconnected and connected pairs of cells recorded from in this study. In Fig. 4 (*A*, *B*, and *C*), the centers of retinal ganglion cell receptive fields are represented as circles (thin lines) that are superimposed on a common stylized geniculate receptive field (thick lines). In *D*, *E*, and *F*, the same arrangement of retinal receptive fields is shown, but with only the center points indicated. Retinal receptive fields that had the same sign (*on* or *off*) as the geniculate cell are shown as either thin solid lines (*B* and *C*) or × (*E* and *F*), whereas retinal receptive fields with the opposite sign are shown as either dashed lines or triangles (*A* and *D*). *A*, *B*, *D*, and *E* in Fig. 4 show the relative receptive-field locations of the retinal ganglion cells and geniculate neurons that did not show peaks in their correlograms. Receptive fields of pairs of cells that showed a monosynaptic peak are illustrated in *C* and *F*. All the retinal cells with connections to geniculate neurons had receptive field centers that overlapped LGN centers by ≥50%. Although all combinations of overlap (center and surround) were present in our data set (Fig. 4, *A*, *B*, *D*, and *E*), only a very small number of cell pairs (Fig. 4, *C*, and *F*) were monosynaptically connected.

The second measure of overlap, the normalized dot product, allowed us to quantify spatial overlap with a single parameter. Figure 5 shows the relationship between presence of connection and degree of spatial overlap. Most important, all pairs of cells with overlap values >0.75 were monosynaptically connected. As the degree of overlap decreased, the percentage of connected cell pairs also decreased, to 50% (for pairs with 0.51–0.75 overlap) and to 9% (for pairs with 0.26–0.50 overlap).

Finally, we examined the relationship between receptive-field overlap and strength of connection by comparing overlap values (the dot product between receptive fields, see METHODS) with values of efficacy and contribution (Fig. 6). Because efficacy and contribution values depend in a complex fashion on the stimulus used (Cleland and Lee 1987; Hubel and Wiesel

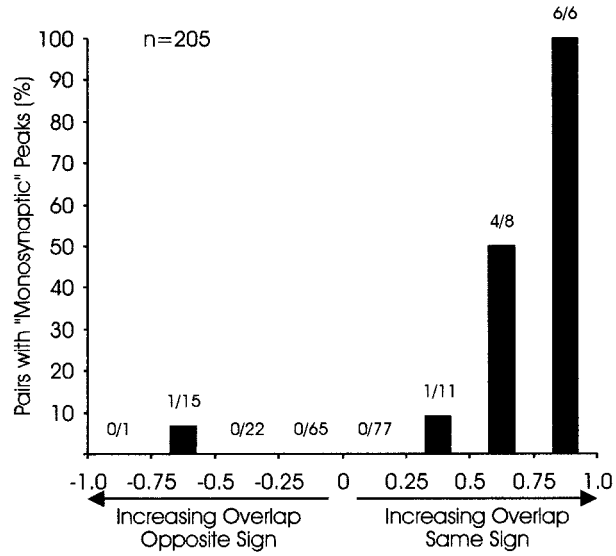

FIG. 5. Relationship between overlap and the probability of a monosynaptic connection. Overlap is measured with the dot-product method and can range from −1.0 to 1.0. The connected fraction—connected cell pairs over the total number in each range—is shown above each histogram bin.

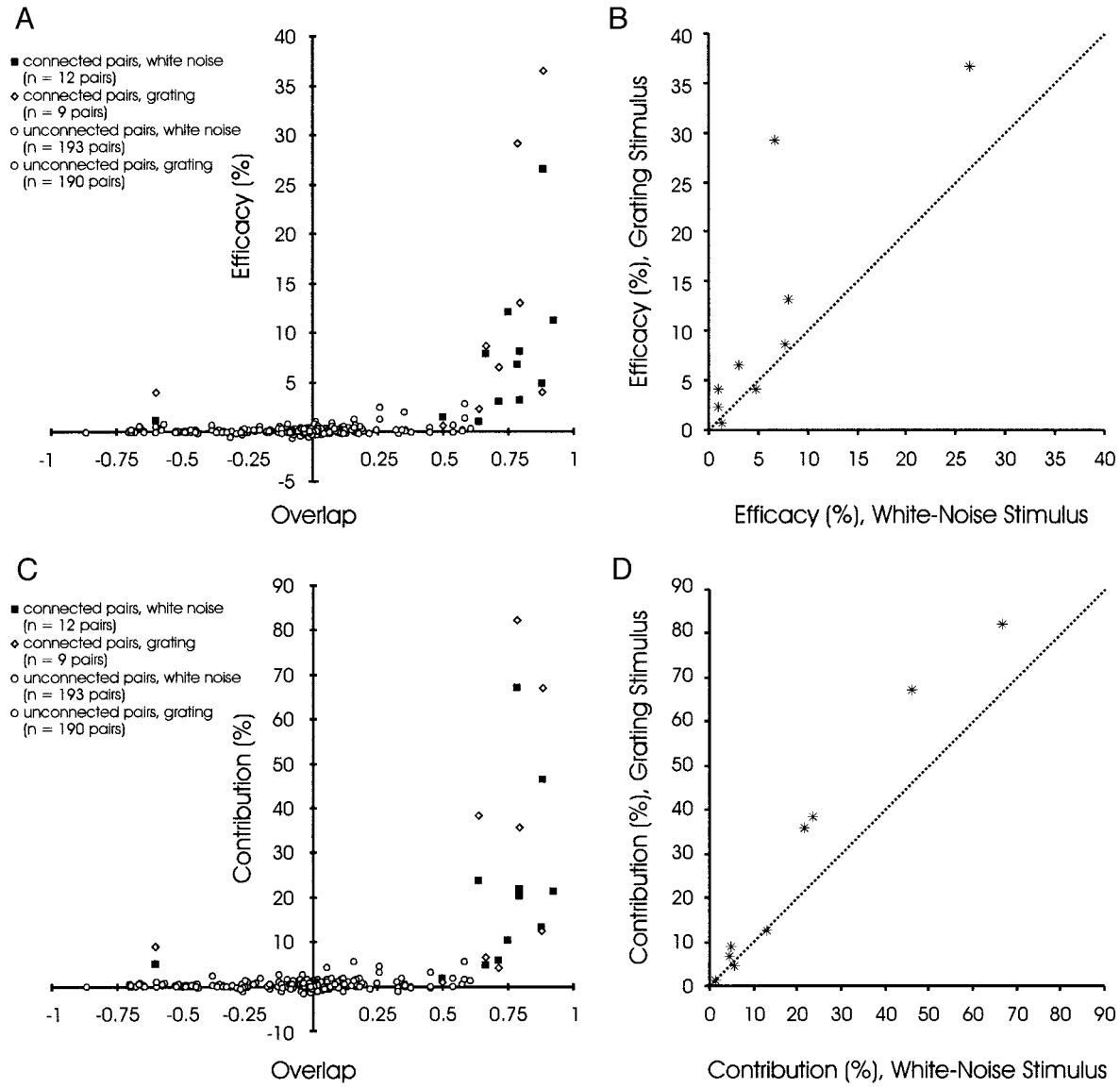

FIG. 6. Relationship between overlap (measured with the dot-product method) and strength of correlation. Correlation strength is expressed either as the efficacy (*A*) or the contribution (*C*) of the retinal neuron in driving the geniculate neuron. Data were collected during white-noise stimulation or, when available, during grating stimulation. *A* and *C*: solid squares indicate values for connected pairs when excited with a white-noise stimulus, shaded diamonds indicate values for connected pairs when excited with a grating stimulus, and open symbols indicate values for unconnected pairs when excited with either stimulus. The few nonzero values for unconnected pairs are from cases in which correlation peaks were too slow (>1 ms) to meet the criteria for monosynaptic connections. *B* and *D*: relationship between efficacy (*B*) and contribution (*D*) for grating stimulation compared with white-noise stimulation.

1961; Kaplan et al. 1987; Lee et al. 1983; Levick et al. 1972), it is necessary to compare values from pairs of cells that are driven by a similar stimulus. The relationship between efficacy and overlap is shown for data collected with grating stimuli (Fig. 6*A*, shaded diamonds) and with white-noise stimuli (Fig. 6*A*, solid squares). Similarly, the relationship between contribution and overlap is shown in Fig. 6*C*. In general, efficacy and contribution values were higher when cells were driven with a grating stimulus compared with a white-noise stimulus (Fig. 6*B* and 6*D*). Under both stimulus conditions, however, there was a clear trend in the relationship between receptive-field overlap and strength of connection: the more complete the spatial overlap, the stronger the connection. A similar relationship between strength of connection and proximity of retinal and geniculate receptive fields is described in Mastronarde (1992). It should be noted that we found cases in which the efficacy or contribution of unconnected pairs (open symbols) were nominally higher than those of a few connected pairs (solid squares or shaded diamonds). This is because the test for monosynaptic connections has an initial stage that rejects correlations slower than approximately 1 ms in width (see METHODS). Several of the retinogeniculate pairs had significant but slower correlations, on the order of several milliseconds. These slower correlations were most likely the result of correlations found within the retina (Mastronarde 1983a) and do not represent monosynaptic connections between retina and LGN.

DISCUSSION

By studying the receptive-field properties and the cross-correlations between retinal ganglion cells and geniculate neurons, we have examined the rules that govern the presence and the strength of individual connections. For strong connections from single ganglion cells, the geniculate receptive field is, of course, very similar to the retinal receptive field, with the same spatial location, response sign (*on* or *off*), and X-Y classification. More significantly, even weakly connected pairs are almost always from same-sign retinal cells with nearby receptive fields. As similarity between receptive fields decreases, so does the likelihood of connection and the strength of connection.

In the following section, we examine three topics: *1*) the technique of cross-correlation analysis as applied to the examination of retinogeniculate connections, *2*) the relationship between specificity, strength, and probability of connections, and *3*) the functional implications of converging and diverging retinogeniculate connections.

Cross-correlation analysis and the retinogeniculate pathway

Cross-correlation analysis has been used extensively in studies of the visual system to examine relationships in the firing patterns of multiple neurons. The location, size and shape of peaks in a cross-correlogram can indicate much about the synaptic circuitry between neurons (Perkel et al. 1967; Usrey and Reid 1999). Although peaks in correlograms can often have multiple causes, correlations between retina and LGN are particularly stereotyped and easy to interpret. Consistent with previous reports (Cleland et al. 1971a,b; Levick et al. 1972; Mastronarde 1987, 1992), retinal ganglion cells and geniculate neurons often displayed peaks in their cross-correlograms, which were quite narrow ($<$1 ms, a slightly lower number than found in previous studies) and occurred with a latency of 2–5 ms ($\sim$2.5 ms for Y-cell inputs, $\sim$4.5 ms for X-cell inputs). These monosynaptic correlations were often stronger ($\leq$83% of the geniculate cell's spikes) than correlations seen in cross-correlograms made between pairs of neurons at other locations in the visual pathway, including pairs of retinal ganglion cells (Mastronarde 1983a,b, 1989; Meister et al. 1995; Rodieck 1967), pairs of geniculate neurons (Alonso et al. 1996; Neuenschwander and Singer 1996; Sillito et al. 1994), geniculate neurons and simple cells in layer 4 of visual cortex (Alonso et al. 1996; Reid and Alonso 1995; Tanaka 1983), or pairs of neurons within the visual cortex (Alonso and Martinez 1998; Singer and Gray 1995; Toyama et al. 1981; Ts'o et al. 1986).

Many features of the pathway from retina to LGN make it ideal for applying cross-correlation analysis to determine the presence and strength of monosynaptic connections. First, the pathway is unidirectional: there is no feedback projection. As a result, the firing of retinal ganglion cells is not influenced by the firing of their targets. Second, estimates of convergence suggest that most geniculate neurons receive input from fewer than six retinal ganglion cells (Cleland et al. 1971a,b; Hamos et al. 1987; Mastronarde 1987, 1992). Peaks in retinogeniculate correlograms therefore tend to be rather large and can be easily distinguished from baseline activity. Third, direct excitatory connections have never been demonstrated between LGN cells, and any correlations between them (Alonso et al. 1996) are therefore likely to be due only to common retinal input (Usrey et al. 1998). Finally, and perhaps most important, it is unlikely that intraretinal correlations would cause positive retinogeniculate correlograms in the absence of a direct connection, as could happen if two ganglion cells were correlated but only one was connected monosynaptically to a given geniculate neuron. Such a "false-positive" retinogeniculate correlation would have the time structure of the intraretinal correlation. However, most correlations between ganglion cells tend to occur over relatively slow time scales (between 2 and 10 ms) compared with the duration of monosynaptic peaks (full width at half-maximum of 0.56 $\pm$ 0.13 ms) seen in retinogeniculate correlograms. This difference in time scale makes it unlikely that our criterion for monosynaptic correlations would yield false positives caused by these slower intraretinal correlations. The one possible exception is for faster (0.5–1.0 ms) correlations seen between neighboring retinal Y cells (Mastronarde 1983b). We do not think these correlations are important in our recordings for two reasons: *1*) they are fairly weak (accounting for $\sim$5% or fewer of the spikes for any pair of Y cells), and *2*) they generally result in a correlogram with *two* narrow peaks that are 2.0 ms apart (Mastronarde 1983b, Fig. 1). Again, because a false-positive retinogeniculate correlation would inherit the structure of the intraretinal correlation, this pattern would be discriminable from the very narrow single peaks we classify as monosynaptic.

Relationship between specificity, strength, and probability of retinogeniculate connections

One way of expressing our findings is that very precise rules determine the connections between retina and LGN. If retinal and geniculate receptive fields are very similar and overlap extensively (overlap value $>$0.75, see Fig. 5), the cells are strongly connected; if the receptive fields differ in any way, the probability of finding connections declines very rapidly, and any connections are weak. The first part of this rule may seem obvious: if a geniculate neuron is receiving most of its excitatory drive from a given retinal cell, the receptive fields are necessarily similar. The second part, however, concerning weaker connections, is not a necessary finding. If a retinal cell contributes only a small percentage of the input to a geniculate neuron, its influence on the geniculate receptive field should be similarly weak. In our sample, however, of the six weakly connected retinogeniculate pairs (contribution $<$15%) all had centers that were overlapped by $\geq$50%, and all but one had the same response sign.

In a similar study of geniculocortical connections (Reid and Alonso 1995), geniculate neurons contributed, on average, 3.1% to the firing of their simple-cell targets in the cortex (maximum 10.3%). In this study, it was found that geniculate neurons with receptive-field centers overlapping the appropriate simple-cell subregion (*on* or *off*) were very likely to be connected to the simple cell. Again, because these connections were relatively weak, none by itself determined a large part of the receptive field structure. The weaker correlations found in the present study are thus similar to those found in the past study of geniculocortical connections: connections were found when the pre- and postsynaptic neurons had similar response properties at the same location, although this need not have been the case.

Functional implications of converging and diverging retinogeniculate connections

Anatomic (Hamos et al. 1987) and physiological (Cleland et al. 1971a; Mastronarde 1987, 1992) estimates of convergence between retinal ganglion cells and geniculate neurons suggest that whereas some geniculate neurons receive input from only one retinal ganglion cell, many others receive converging input from two or more ganglion cells. In the geniculocortical pathway, one role for convergence is clearly the transformation of receptive field properties: layer 4 simple cells, which have elongated, orientation-selective receptive fields with separate *on* and *off* subregions, receive convergent input from geniculate neurons with receptive fields that overlap the length of the subregions (Hubel and Wiesel 1962; Reid and Alonso 1995; see also Chapman et al. 1991; Ferster et al. 1996). In the pathway from retina to LGN, the role of convergence is much less clear.

A geniculate surround is usually stronger than the surrounds of its retinal inputs (Hubel and Wiesel 1961). Inhibitory influences—which are difficult to assess in cross-correlation studies but have been characterized with intracellular recordings (Singer and Creutzfeldt 1970; Singer et al. 1972)—are likely to play a role in the stronger surround. It is also possible that geniculate neurons receive convergent input from retinal ganglion cells with centers that are opposite in sign but overlap the surround of the geniculate receptive field (suggested by Hubel and Wiesel 1961 and Maffei and Fiorentini 1971). In the present study and others (Cleland et al. 1971a,b; Mastronarde 1987, 1992), however, monosynaptic connections between retinal ganglion cells and geniculate neurons the centers of which have opposite signs have been encountered rarely. Of the many pairs of neurons we studied with opposite-sign receptive fields (Fig. 4, *A*, and *D*), only one was weakly connected (Figs. 2, pair 135; and 4, *C*, and *F*).

Although it cannot be ruled out that convergence between retina and LGN is simply a result of incomplete pruning of aberrant connections during development, convergence may also be important in the transmission of information from retina to LGN. One possible role of convergence of several retinal cells onto one geniculate neuron depends critically on divergence in the same pathway. Estimates from anatomic studies in the cat (reviewed in Cleland 1986) suggest that axons from individual retinal X cells diverge to contact at least three geniculate neurons; Y cells diverge by a factor of at least 30. Results from our study suggest that branching axons should most strongly innervate geniculate neurons with very similar receptive fields and weakly innervate a subset of the geniculate neurons with receptive fields that only partially overlap or that differ in receptive-field type (X or Y) or sign (*on* or *off*). As had been predicted by Cleland (1986), a recent study found that pairs of geniculate neurons with very similar receptive fields often had strong and narrow peaks (~1 ms) in their cross-correlograms, centered at time zero (Alonso et al. 1996). These correlograms provided strong evidence for the presence of common input. The same study also described smaller peaks, which occurred less frequently, between pairs of geniculate neurons that had receptive fields that were either partially overlapped or were mismatched: X and Y or *on* and *off*. Taken together, it seems likely that a retinal ganglion cell with a receptive field similar to and well overlapped with two geniculate cells almost certainly provides strong input to those cells, while simultaneously providing weak input to a subset of other geniculate cells that are less similar. Thus divergence in the pathway from retina to LGN establishes small ensembles of geniculate neurons that fire a variable proportion of their spikes in tight synchrony.

As we have previously argued (Alonso et al. 1996, Usrey and Reid 1999), synchronous activity in the LGN—caused by divergent connections from the retina (Usrey et al. 1998)—may serve several purposes. In development, geniculate synchrony may be important for the patterning of geniculocortical connections (cf. Erwin and Miller 1998; Meister et al. 1991; Miller 1994). In the adult, synchronous geniculate spikes can be used to derive more information about the visual stimulus (Dan et al. 1998). Finally, perhaps the most important consequence of synchronous activity in the LGN stems from the fact that many LGN cells provide convergent input to individual layer 4 simple cells in area 17 (Reid and Alonso 1995; see Peters and Payne 1993). Some of these inputs come from tightly synchronized pairs of LGN cells, and these synchronous inputs have been shown to be especially effective in driving layer 4 simple cells (Alonso et al. 1996). Thus divergence from retina to LGN and reconvergence from LGN to layer 4 may act as a means to enhance the transfer of visual information from the retina to cortex.

We thank E. Serra for expert technical assistance and D. Hubel, M. Livingstone, S. M. Sherman, and M. Hawken for insightful comments on the manuscript.

This work was supported by National Eye Institute Grants EY-06604, EY-10115, and EY-12196; The Klingenstein Fund; The Harvard Mahoney Neuroscience Institute; and The Howard Hughes Medical Institute.

Present address of W. M. Usrey: Center for Neuroscience, University of California, 1544 Newton Court, Davis, CA 95616.

Address reprint requests to: R. C. Reid, Dept. of Neurobiology, Harvard Medical School, 220 Longwood Ave. Boston, MA 02115.

Received 7 January 1999; accepted in final form 30 July 1999.

REFERENCES

ALONSO, J.-M. AND MARTINEZ, L. Functional connectivity between simple cells and complex cells in cat visual cortex. *Nat. Neurosci.* 1: 395–403, 1998.

ALONSO, J.-M., USREY, W. M., AND REID, R. C. Precisely correlated firing in cells of the lateral geniculate nucleus. *Nature* 383: 815–819, 1996.

ARNETT, D. W. Correlation analysis of units recorded in the cat dorsal lateral geniculate nucleus. *Exp. Brain Res.* 22: 111–130, 1975.

BISHOP, P. O., BURKE, W., AND DAVIS, R. Synapse discharge by single fibre in mammalian visual system. *Nature* 128: 728–730, 1958.

BISHOP, P. O., BURKE, W., AND DAVIS, R. The interpretation of the extracellular response of single lateral geniculate cells. *J. Physiol. (Lond.)* 162: 451–472, 1962.

CHAPMAN, B., ZAHS, K. R., AND STRYKER, M. P. Relation of cortical cell orientation selectivity to alignment of receptive fields of the geniculocortical afferents that arborize within a single orientation column in ferret visual cortex. *J. Neurosci.* 11: 1347–1358, 1991.

CITRON, M. C., EMERSON, R. C., AND IDE, L. S. Spatial and temporal receptive-field analysis of the cat's geniculocortical pathway. *Vision Res.* 21: 385–396, 1981.

CLELAND B. G. The dorsal lateral geniculate nucleus of the cat. In: Visual Neuroscience, edited by J.D. Pettigrew, K.S. Sanderson, and W.R. Levick. London: Cambridge Univ. Press, 1986, p. 111–120.

CLELAND, B. G. AND LEE, B. B. A comparison of visual responses of cat lateral geniculate nucleus neurones with those of ganglion cells afferent to them. *J. Physiol. (Lond.).* 369: 249–268, 1985.

CLELAND, B. G., DUBIN, M. W., AND LEVICK, W. R. Simultaneous recording of input and output of lateral geniculate neurones. *Nat. New Biol.* 231: 191–192, 1971a.

CLELAND, B. G., DUBIN, M. W., AND LEVICK, W. R. Sustained and transient neurones in the cat's retina and lateral geniculate nucleus. *J. Physiol. (Lond.)* 217: 473–496, 1971b.

DAN, Y., ALONSO, J.-M., USREY, W. M., AND REID, R. C. Coding of visual information by precisely correlated spikes in the LGN. *Nat. Neurosci.* 1: 501–507, 1998.

ECKHORN, R. AND THOMAS, U. A new method for the insertion of multiple microprobes into neural and muscular tissue, including fiber electrodes, fine wires, needles and microsensors. *J. Neurosci. Methods* 49: 175–179, 1993.

ENROTH-CUGELL, C. AND ROBSON, J. G. The contrast sensitivity of retinal ganglion cells of the cat. *J. Physiol. (Lond.)* 187: 517–552, 1966.

ERWIN, E. AND MILLER, K. D. Correlation-based development of ocularly matched orientation and ocular dominance maps: determination of required input activities. *J. Neurosci.* 18: 9870–9895, 1998.

FERSTER, D., CHUNG, S., AND WHEAT, H. Orientation selectivity of thalamic input to simple cells of cat visual cortex. *Nature.* 380: 249–252, 1996.

FREYGANG, W. H., JR. An analysis of extracellular potentials from single neurons in the lateral geniculate nucleus of the cat. *J. Gen. Physiol.* 41: 543–564, 1958.

FUKADA, Y. Receptive field organization of cat optic nerve fibers with special reference to conduction velocity. *Vision Res.* 11: 209–26, 1971.

GIELEN, C.C.A.M., VAN GISBERGEN, J.A.M., AND VENDRI, A.J.H. Reconstruction of cone-system contributions to responses of colour-opponent neurones in monkey lateral geniculate. *Biol. Cybern.* 44: 211–221, 1982.

GUIDO, W., LU, S.-M., AND SHERMAN, S. M. Relative contributions of burst and tonic responses to the receptive field properties of lateral geniculate neurons in the cat. *J. Neurophysiol.* 68: 2199–2211, 1992.

GUIDO, W. AND WEYAND, T. G. Burst responses in lateral geniculate neurons of the awake behaving cat. *J. Neurophysiol.* 74: 1782–1786, 1995.

HAMOS, J. E., VAN HORN, S. C., RACZKOWSKI, D., AND SHERMAN, S. M. Synaptic circuits involving an individual retinogeniculate axon in the cat. *J. Comp. Neurol.* 259: 165–192, 1987.

HUBEL, D. H. Single unit activity in lateral geniculate body and optic tract of unrestrained cats. *J. Physiol. (Lond.)* 150: 91–104, 1960.

HUBEL, D. H. AND WIESEL, T. N. Integrative action in the cat's lateral geniculate body. *J. Physiol. (Lond.)* 155: 385–398, 1961.

HOCHSTEIN, S. AND SHAPLEY, R. M. Quantitative analysis of retinal ganglion cell classifications. *J. Physiol. (Lond.)* 262: 237–264, 1976.

IKEDA, H. AND WRIGHT, M. J. Receptive field organization of "sustained" and "transient" retinal ganglion cells which subserve different function roles. *J. Physiol. (Lond.)* 227: 769–800, 1972.

JONES, J. P. AND PALMER, L. A. The two-dimensional spatial structure of simple receptive fields in cat striate cortex. *J. Neurophysiol.* 58: 1187–211, 1987.

KAPLAN, E., PURPURA, K., AND SHAPLEY, R. M. Contrast affects the transmission of visual information through the mammalian lateral geniculate nucleus. *J. Physiol. (Lond.)* 391: 267–288, 1987.

KAPLAN, E. AND SHAPLEY, R. The origin of the S (slow) potential in the mammalian lateral geniculate nucleus. *Exp. Brain Res.* 55: 111–116, 1984.

KUFFLER, S. Discharge patterns and functional organization of mammalian retina. *J. Neurophysiol.* 16: 37–68, 1953.

LEE, B. B., VIRSU, V., AND CREUTZFELDT, O. D. Linear signal transmission from prepotentials to cells in the macaque lateral geniculate nucleus. *Exp. Brain Res.* 52: 50–56, 1983.

LEVICK, W. R., CLELAND, B. G., AND DUBIN, M. W. Lateral geniculate neurons of cat: retinal inputs and physiology. *Invest. Opthalmol.* 11: 302–311, 1972.

LINSENMEIER, R. A., FRISHMAN, L. J., JAKIELA, H. G., AND ENROTH-CUGELL, C. Receptive field properties of X and Y cells in the cat retina derived from contrast sensitivity measures. *Vision Res.* 22: 1173–1183, 1982.

LIVINGSTONE, M. S., AND HUBEL, D. H. Effects of sleep and arousal on the processing of visual information in the cat. *Nature* 291: 554–561, 1981.

LU, S.-M., GUIDO, W., AND SHERMAN, S. M. Effects of membrane voltage on receptive field properties of lateral geniculate neurons in the cat: contributions of the low-threshold Ca^{2+} conductance. *J. Neurophysiol.* 68: 2185–2198, 1992.

MAFFEI, L. AND FIORENTINI, A. Retinogeniculate convergence and analysis of contrast. *J. Neurophysiol.* 35: 65–72, 1971.

MASTRONARDE, D. N. Correlated firing of cat retinal ganglion cells. I. Spontaneously active inputs to X- and Y-cells. *J. Neurophysiol.* 49: 303–324, 1983a.

MASTRONARDE, D. N. Interactions between ganglion cells in cat retina. *J. Neurophysiol.* 49: 350–365, 1983b.

MASTRONARDE, D. N. Two classes of single-input X-cells in cat lateral geniculate nucleus. II. Retinal inputs and the generation of receptive-field properties. *J. Neurophysiol.* 57: 381–413, 1987.

MASTRONARDE, D. N. Correlated firing of retinal ganglion cells. *Trends Neurosci.* 12: 75–80, 1989.

MASTRONARDE, D. N. Nonlagged relay cells and interneurons in the cat lateral geniculate nucleus: receptive-field properties and retinal inputs. *Vis. Neurosci.* 8: 407–441, 1992.

MEISTER, M., LAGNADO, L., AND BAYLOR, D. A. Concerted signaling by retinal ganglion cells. *Science* 270: 1207–1210, 1995.

MEISTER, M., WONG, R. O., BAYLOR, D. A., AND SHATZ, C. J. Synchronous bursts of action potentials in ganglion cells of the developing mammalian retina. *Science* 252: 939–943, 1991.

MILLER, K. D. A model for the development of simple cell receptive fields and the ordered arrangement of orientation columns through activity-dependent competition between ON- and OFF-center inputs. *J. Neurosci.* 14: 409–441, 1994.

MUKHERJEE, P. AND KAPLAN, E. Dynamics of neurons in the cat lateral geniculate nucleus: in vivo electrophysiology and computational modeling. *J. Neurophysiol.* 74: 1222–1243, 1995.

NEUENSCHWANDER, S., AND SINGER, W. Long-range synchronization of oscillatory light responses in the cat retina and lateral geniculate nucleus. *Nature* 379: 728–32, 1996.

PERKEL, D. H., GERSTEIN, G. L., AND MOORE, G. P. Neuronal spike trains and stochastic point processes. II. Simultaneous spike trains. *Biophys. J.* 7: 419–440, 1967.

PETERS, A. AND PAYNE, B. R. Numerical relationships between geniculocortical afferents and pyramidal cell modules in cat primary visual cortex. *Cereb. Cortex.* 3: 69–78, 1993.

REID, R. C. AND ALONSO, J. M. Specificity of monosynaptic connections from thalamus to visual cortex. *Nature* 378: 281–284, 1995.

REID, R. C. AND SHAPLEY, R. M. Spatial structure of cone inputs to receptive fields in primate lateral geniculate nucleus. *Nature* 356: 716–718, 1992.

REID, R. C., VICTOR, J. D., AND SHAPLEY, R. M. The use of m-sequences in the analysis of visual neurons: linear receptive field properties. *Vis. Neurosci.* 16: 1015–1027, 1997.

RODIECK, R. W. Quantitative analysis of cat retinal ganglion cell response to visual stimuli. *Vision Res.* 5: 583–601. 1965.

RODIECK, R. W. Maintained activity of cat retinal ganglion cells. *J. Neurophysiol.* 30: 1043–1071. 1967.

SAUL, A. B. AND HUMPHREY, A. L. Spatial and temporal response properties of lagged and non-lagged cells in the cat lateral geniculate nucleus. *J. Neurophysiol.* 64: 206–224. 1990

SHERMAN, S. M. Dual response modes in lateral geniculate neurons: Mechanisms and functions. *Vis. Neurosci.* 13: 205–213, 1996.

SHERMAN, S. M. AND KOCH, C. The control of retinogeniculate transmission in the mammalian lateral geniculate nucleus. *Exp. Brain Res.* 63: 1–20. 1986.

SILLITO, A. M., JONES, H. E., GERSTEIN, G. L., AND WEST, D. C. Feature-linked synchronization of thalamic relay cell firing induced by feedback from the visual cortex. *Nature* 369: 479–82, 1994.

SINGER, W. AND CREUTZFELDT, O. D. Reciprocal lateral inhibition of on- and off-center neurones in the lateral geniculate body of the cat. *Exp. Brain Res.* 10: 311–330, 1970

SINGER, W. AND GRAY, C. M. Visual feature integration and the temporal correlation hypothesis. *Annu. Rev. Neurosci.* 18: 555–586, 1995.

SINGER, W., PÖPPEL, E., AND CREUTZFELDT, O. Inhibitory interaction in the cat's lateral geniculate nucleus. *Exp. Brain Res.* 14: 210–226, 1972.

SO, Y. T. AND SHAPLEY, R. M. Spatial tuning of cells in and around lateral geniculate nucleus of the cat: X and Y relay cells and perigeniculate interneurons. *J. Neurophysiol.* 45: 107–120, 1981.

STERIADE, M., MCCORMICK, D. A., AND SEJNOWSKI, T. J. Thalamocortical oscillations in the sleeping and aroused brain. *Science.* 262: 679–685, 1993.

SUTTER, E. E. A practical non-stochastic approach to nonlinear time-domain analysis. In: *Advanced Methods of Physiological Systems Modeling,* edited by V. Marmarelis. Los Angeles: University of Southern California, 1987, vol. 1, p. 303–315.

SUTTER, E. E. A deterministic approach to nonlinear systems analysis. In: *Nonlinear Vision*: *Determination of Neural Receptive Fields, Function, and Networks.* Edited by R. Pinter and B. Nabet. Cleveland, OH: CRC, 1992, p. 171–220.

TANAKA, K. Organization of geniculate inputs to visual cortical cells in the cat. *Vision Res.* 25: 357–364, 1985.

TOYAMA, K., KIMURA, M., AND TANAKA, K. Cross-correlation analysis of interneuronal connectivity in cat visual cortex. *J. Neurophysiol.* 46: 191–201, 1981.

TS'O, D. Y., GILBERT, C. D., AND WIESEL, T. N. Relationships between horizontal interactions and functional architecture in cat striate cortex as revealed by cross-correlation analysis. *J. Neurosci.* 6: 1160–1170, 1986.

USREY, W. M., AND REID, R. C. Synchronous activity in the visual system. *Annu. Rev. Physiol.* 61: 435–456, 1999.

USREY, W. M., REPPAS, J. B., AND REID, R. C. Paired-spike interactions and synaptic efficacy of retinal inputs to thalamus. *Nature* 395: 384–387, 1998.

WOLFE, J. AND PALMER, L. A. Temporal diversity in the lateral geniculate nucleus of cat. *Vis. Neurosci.* 15: 653–675, 1998.